Appendix DR1

Intense and widespread seismicity during the end-Triassic mass extinction due to emplacement of a large igneous province

Sofie Lindström[1*], Gunver Krarup Pedersen[1], Bas van de Schootbrugge[2], Katrine Hovedskov Hansen[3], Natascha Kuhlmann[4], Jean Thein[4], Leif Johansson[5], Henrik Ingermann Petersen[6], Carl Alwmark[5], Karen Dybkjær[1], Rikke Weibel[1], Mikael Erlström[7], Lars Henrik Nielsen[1], Wolfgang Oschmann [8], Christian Tegner [9]

Expanded methods

Sedimentology and sampling: Sedimentological logs were measured in the N Albert quarry in southern Sweden and in cored sections from deep wells in the Stenlille area in eastern Denmark, as well as the Rødby-1 core in southern Denmark (Figs. 2, DR1–DR2). Similarly, the Schandelah and Mariental cores from Germany, the Grouft core and a temporary road construction outcrop Junglinster Heedhaff in Luxembourg, were measured and logged (Figs. 2, DR3). Drillcore sampling of the Luxembourg material was carried out at the Service Géologique Luxembourg and laboratory analyses at the Steinmann-Institute (University of Bonn). The interpretation of the depositional environments is supported by detailed studies of the palynology, coal petrology, stable isotope geochemistry and wire-line log motifs (Nielsen 2003; Lindström and Erlström, 2006; van de Schootbrugge et al. 2009; Heunisch et al. 2010; Lindström et al. 2012; Kuhlmann et al., 2013).

Soft-sediment deformations: Seismic shaking effects on sediments can result in both gravity driven phenomena, and the development of specific sedimentary structures, seismites (*sensu* *stricto*) (Montentat et al., 2007). Gravitational disturbances include various types of mass movement of sediments or rocks, e.g. mud-flows, debris-flows, turbidites, slumps, slides and rock falls. Some of these may occur on very gentle slopes along basin margins and may be caused by seismic events, but can also be caused by storms, salt or mud intrusions (Montenat et al., 2007). A variety of other processes that cause sudden increases of pore pressure in the sediment, including slope instability, overloading of water or sediments that increase pore pressure in the sediment, differential loading, wave-induced stresses or sudden changes in groundwater level can also induce soft-sediment deformations (Owen, 1996; Collinson et al., 2006).

Soft sediment deformation structures include load structures, slump folds, and a range of water escape structures. Many soft sediment deformation structures are syn-depositional or have formed shortly after deposition, before compaction. A shock applied to waterlogged, loosely packed sediment can change the packing and, in the process, increase the fluid pressure to the extent that the sediment undergoes temporary liquefaction. In this condition the sediment deforms readily (Collinson et al., 2006). After expulsion of pore water the sediments becomes less porous and thus less susceptible to liquefaction. Consequently a later shock is likely to fluidize only the sediments deposited after the last shock.

The soft-sediment deformation structures have been studied in cores and outcrops, and are exemplified in Figs. 2, DR4 and DR5. The seismites are distinguished from load structures on basis of petrography (minimal contrast in grain-size and sorting between the beds with deformation structures and the undeformed beds above and below) and great lateral continuity. The latter applies to seismite 1 in the N Albert quarry, where a mudstone and the overlying sandstone are deformed. In the quarry the deformation structures are not local, but are laterally continuous within the quarry, 50–100 m.

Palynology: For palynology, ca 20 g of bulk rock was treated in alternating steps with hydrochloric (38%) and hydrofluoric acid (40%) to remove carbonate and silicate mineral phases. After washing to neutrality, residues were sieved with 11 µm mesh-size sieves and mounted on strew slides. Up to 300 palynomorphs were counted per slide with a compound microscope at 650x magnification. Abundance data were calculated as percentages of total palynomorph assemblage.

Geochemistry, Organic C-isotopes: The sedimentary rock samples were treated with HCl prior to carbon isotopic analysis to remove all carbonate. The residues were rinsed several times with distilled water, dried for 3 days at 80°C and subsequently ground to a homogeneous powder using an agate mortar. Depending on their TOC content sample aliquots of 3–10 mg were weighed and wrapped into tin capsules. At least two aliquots were prepared per sample. Carbon isotope analysis of TOC was subsequently performed using a Flash Elemental Analyzer 1112 (Thermoquest), connected to the continuous flow inlet system of a MAT gas source mass spectrometer (Thermoquest) at the Institute of Geosciences (Goethe University Frankfurt). USGS 24 standard was analyzed along with the samples in order to prove for accuracy and precision. Both samples and standards reproduced within ±0.2‰. Approximately 0.5 grams each of additional samples were analyzed by EA-IRMS at Iso-Analytical Laboratory in Cheshire, UK. The samples were decarbonized with 1M HCl to remove all carbonate, and the residues were washed twice with destilled water and subsequently dried at 60°C prior to isotope analysis.

Geochemistry, INAA analysis: Finely milled samples were treated by a nickel-sulphide fire assay (fusion at approximately 1000°C of finely milled sample mixed with Ni, S, $Na_2B_4O_7$, Na_2CO_3,

SiO_2) for pre-concentration of the platinum group elements prior to determination by neutron activation analysis (NAA) at Becquerel Laboratories, Canada. Detection limits were 1 ppb for Au, 1 ppb for Ir, 10 ppb for Os, 20 ppb for Pd, 20 ppb for Pt, 5 ppb for Rh and 50 ppb for Ru. The results are presented in Table DR1.

Shock metamorphism: For the shock metamorphic study; six thin sections were prepared from material from seismite 1 and 2 from the N Albert quarry. The thin sections were then studied using a Leitz 5-axes universal stage mounted on an optical microscope. No shock metamorphic features were observed.

Additional Swedish localities with soft-sediment deformation

Apart from the extensive soft-sediment deformations at the top of the Bjuv Member and within the Boserup beds at the N Albert quarry (Fig. DR1), such structures have also been recorded from other localities in Scania, southern Sweden. The Fleninge 266 core, drilled 1935 in the village Fleninge (Fig. DR1), penetrated 180 m of Lower Jurassic and Rhaetian strata of the Rya Formation and the Höganäs Formation, the latter including the Helsingborg, Bjuv and Vallåkra Members in descending order (Troedsson, 1951). Unfortunately only a selected number of core samples have been preserved, and these are housed at the Department of Geology, Lund University. The Triassic–Jurassic boundary, as defined by the first occurrence of *Cerebropollenites thiergartii* is located within the lower part of the Helsingborg Member (at 132.87–132.49 m; Lindström and Erlström, 2006). At this level the first occurrence of *Kraeuselisporites reissingerii* and the first common occurrence of *Pinuspollenites minimus* are also registered. The last common occurrence of *Ricciisporites tuberculatus* is within the lower part of the Boserup beds (at 148.60 m), but it should be noted that no samples have been preserved from the upper part of the Boserup beds (Lindström and Erlström, 2006). The same sample also displays a very distinct soft-sediment deformation, i.e. located ca 3.4 m above the top coal. A sample just above the top of the Boserup beds is dominated by trilete spores, and is regarded as transitional between the latest Rhaetian *Ricciisporites–Polypodiisporites* Zone (Lund, 1977) and the Hettangian *Pinuspollenites–Trachysporites* Zone (Lund, 1977). The last record of the marine dinoflagellate cyst *Rhaetogonyaulax rhaetica* is within the so called "roof clay", a light grey kaolinite rich clay that marks the top of the Bjuv Member in the Fleninge 266 core (Lindström and Erlström, 2006; Troedsson, 1951). The last common occurrence of *R. rhaetica* is however, lower within the Bjuv Member (at 156.92–156.80 m) and this is interpreted to correlate with MFS7 shales (Lindström and Erlström, 2006).

In the cored 1.1008 borehole drilled in the northern part of the city Helsingborg the almost 42 m thick TJ-boundary succession contains a grey siltstone interval similar to that in the Stenlille cores, and which constitutes the more distal equivalent of the Boserup beds. Within this interval there are several levels of soft-sediment deformations. The grey siltstone interval contains a palynoflora assigned to the *Ricciisporites–Polypodiisporites* Zone.

Seismites vs. dinosaur footprints

Terrestrial TJ-boundary strata of southern Sweden are known to contain dinosaur tracks assigned to the ichnotaxon *Kayenthapus* (Ahlberg and Siverson, 1991; Gierliński and Ahlberg, 1994; Vajda et al. 2013). Cross-sections of soft-sediment deformations caused by vertebrate tracks from the late Triassic of Greenland (Milàn et al. 2007) show much smaller sized deformations, different in shape and form to the soft-sediment deformations in the N Albert quarry. In addition, Lower Jurassic paralic strata at the coastal cliffs of Sose Bugt, Bornholm, also contain large dinosaur tracks, preserved in cross-section. These are steep-walled, concave-to-flat-bottomed depressions, with a raised ridge at each side of the walls. Where visible, the infillings are laminated, draping the contours of the bottom of the depression (Clemmensen et al. 2014). The soft-sediment deformations found in the N Albert quarry were carefully investigated. They lack the steep walls and the raised ridges, and have no features which suggest an origin from dinosaur activity.

Stratigraphy of the Luxembourg localities

In the NE Paris Basin (Trier-Luxembourg Embayment) Rhaetian sediments reach thicknesses of 28 m just south of the Luxembourg-France border (drillcore Boust) to less than 4 m in Central Luxembourg and the southern Eifel (Germany). The Rhaetian succession is subdivided in two major facies. The lower one, traditionally called “Sables de Mortinsart” consists of conglomerate bearing light to greenish grey sandstones and siltstones interbedded by dark grey to black silt-streaked clays. These beds correspond biostratigraphically to the Contorta beds. They grade into silty clays, the color of which normally turns from medium grey at the basis to brownish red in the upper part. Locally the brownish red clays may be missing. This clay sequence is defined as “Argiles de Levallois”, (stratigraphically: Triletes beds). They are overlain by bituminous dark gray marls of the lowest Hettangian which contain fully marine fossils.

Lithostratigraphically the sharp change from the Argiles de Levallois to the calcareous fossil bearing marls corresponds to the Triassic–Jurassic boundary (Muller, 1974). Others (e.g. Rauscher et al. 1995) separate the upper Argiles de Levallois as “Transition Beds”. The top of the Argiles de Levallois in the Luxembourgian and French sections lies exactly below the $\delta^{13}C_{org}$ negative excursion 2, which was observed in the drillcore Boust (Kuhlmann et al. 2013).

Paleogeographically the NE Paris Basin was a narrow gulf bordered to the west by the London-Brabant Massif and to the east by the Rhenish Massif. During the deposition the environment changed from shallow marine to lagoonal. In nearly all Luxembourgian drillcores and outcrops one to three horizons with soft sediment deformations are observed. As example Fig. S6 shows soft sediment deformations in the drill core Grouft (Fig. DR5A–C), north of Luxembourg City and the outcrop Junglinster Heedhaff (Fig. DR5D–E) about 20 km east of Luxembourg City. In the Grouft core three clearly defined horizons of micro-slumping and micro-folding appear in the upper part of the Argiles de Levallois (Triletes beds), at a depth of 91,50–92,90 m, 2 m below the ETE. Another type of deformation can be observed in the outcrop Junglinster Heedhaff in a depth of 1,50 m and 2,50 m. An alternation of black clays and whitish quartzites displays very clear water escape structures and microfolded quartzite bands. It is overlain by a completely unsorted black conglomerate with a sand-clay matrix, which develops to the top into sheared and folded sand layers displaying a flamed structure. They finally are injected into laminated reddish grey clays which are microslumped (Fig. DR5D–E). The uppermost slump horizon lies about 2 m below the Lower Jurassic marls.

Magnetostratigraphic correlations

Hounslow et al. (2007) offer two alternatives for magnetostratigraphic correlation between the TJB of St. Audrie's Bay in the UK and the Newark Supergroup (Kent et al., 1995; Kent and Olsen, 1999). They correlate the magnetic reversal E23r in the Newark Supergroup either with the SA5r reversal in the lower part of the Blue Lias Formation, or with either/or both of the thin reversals SA5n.2r or 3r in the upper Westbury Formation and lowermost Lilstock Formation, respectively (Hounslow et al., 2004). They argue that the latter option is better supported by the palynological turnovers in these two sections (Hounslow et al., 2007). Whiteside et al. (2007; figure 4 therein) indirectly accept this correlation in their figured material. Deenen et al. (2010, 2011) also favour this interpretation.

Other localities with disturbed TJ-boundary strata

Kamień Pomorski IG-1, Poland (locality 12 on Fig. 1): There are two levels of disturbed strata just below and above the inferred TJ-boundary in the Kamień Pomorski IG-1, Poland (Pieńkowski et al., 2012). The palynoflora within the interval with the disturbed strata contains *Ricciisporites tuberculatus* (low numbers but restricted to this interval), dominant *Limbosporites lundbladiae* and *Cingulizonates rhaeticus*, common *Ovalipollis ovalis* and *Concavisporites. Cerebropollenites thiergartii* has its first occurrence at the top of the interval (Pieńkowski et al., 2012).

Csővár section, Hungary (locality 13 on Fig. 1): Several layers of slump balls and slump structures have been registered within the 15.80–28.5m interval, as well as one additional level at 36m, of the Csővár section (Pálfy et al., 2007). The 15.8–28.5 m interval is stratigraphically constrained between the last occurrence of Triassic foraminifera and the first occurrence of a psiloceratid ammonoid (Pálfy et al., 2007).

Furkaska section, Slovakia (locality 14 on Fig. 1): A layer with soft-sediment deformation is present within the upper part of the Fatra Formation in the Furkaska section (Michalik et al., 2012). Palynologically, the Fatra Formation contains abundant *Ricciisporites tuberculatus* and is correlated with the *Ricciisporites–Polypodiisporites* Zone (Lund, 1977).

Southern Alps, Italy (locality 15 on Fig. 1): In the Southern Alps slump beds appear restricted to the lower part of the Malanotte Formation (Galli et al. , 2007) which can be assigned a Rhaetian age based on the presence of *Rhaetipollis germanicus*. In some sections a negative $\delta^{13}C_{carb}$-isotope excursion is present in the lowermost part of the Malanotte Formation, and generally there is a similar sized excursion at its top (Galli et al., 2005).

Lovède Basin, southern France (locality 16 on Fig. 1): Disturbed upper Rhaetian strata interpreted as tsunami deposits triggered by seismic activity were reported from the Upper Member of the Rhaetian Formation in the Pégairolles de l'Escalette section in the Lovède Basin (20). The Upper Member is preceded by beds containing *Avicula contorta* within the Unité Supérieure of the Lower Member, and the last occurrence of *Rhaetogonyaulax rhaetica* is within the the lower part of the Upper Member (Courtinat and Piriou, 2002; Courtinat et al., 2003).

References

Ahlberg, A., and Siverson, M., 1991, Early Jurassic dinosaur footprints in Helsingborg, southern Sweden: GFF, vol. 113, p. 339–340.

Clemmensen, L.B., Milàn, J., Pedersen, G.K., Johannesen, A.B., and Larsen, C., 2014, Dinosaur tracks in Lower Jurassic coastal plain sediments (Sose Bugt Member, Rønne Formation) on Bornholm, Denmark: Lethaia, Vol. 47, pp. 485–493. DOI: 10.1111/let.12073.

Collinson, J., Mountney, N., and Thompson, D., 2006, Sedimentary structures, 3rd edition:Terra Publishing, England, 292 p.

Courtinat, B., and Piriou, S., 2002, Palaeoenvironmental distribution of the Rhaetian dinoflagellate cysts *Dapcodinium priscum* EVITT, 1961, emend. Below, 1987 and *Rhaetogonyaulax rhaetica* (SARJEANT) LOEBLICH and LOEBLICH, 1976, emend. Harland et al., 1975, emend. Below, 1987: Geobios, vol. 35, p. 429–439.

Courtinat, B., Piriou, S., and Rio, M., 2003, Phytoclasts in palynofacies definition: the example of Rhaetian sedimentary organic matter in SE France: Revue de Micropaléontologie, vol. 46, p. 11–21.

Galli, M.T., Jadoul, F., Bernasconi, S.M., and Weissert, H., 2005, Anomalies in global carbon cycling and extinction at the Triassic/Jurassic boundary: evidence from a marine C-isotope record: Palaeogeography, Palaeoclimatology, Palaeoecology, vol. 216, p. 203–214.

Galli, M.T., Jadoul, F., Bernasconi, S.M., Cirilli, S., and Weissert, H., 2007, Stratigraphy and palaeoenvironmental analysis of the Triassic–Jurassic transition in the western Southern Alps (Northern Italy): Palaeogeography, Palaeoclimatology, Palaeoecology: vol. 244, p. 52–70.

Gierliński, G., and Ahlberg, A., 1994, Late Triassic and Early Jurassic dinosaur footprints in the Höganäs Formation of southern Sweden.: Ichnos, vol. 3, p. 99–105.

Heunisch, C., Luppold, F.W., Reinhardt, L. and Röhling, H.-G., 2010, Bio-, und lithostratigraphie im Grenzbereich Trias/Juras in ger Bohrung Mariental 1 (Lappwaldmulde, Ostniedersachsen): Zeitschrift der Deutches Geologischen Gesellschaft, vol. 161, p. 51-98.

Kuhlmann, N., Thein, J., Fiebig, J., and Nagel, T., 2013, Analysis of the environmental changes from the Upper Triassic to the Lower Jurassic (T/J Boundary Event in the NE Paris Basin): Geofluids 2013, Tübingen, Germany.

Lindström, S., van de Schootbrugge, B., Dybkjær, K., Pedersen, G.K., Fiebig, J., Nielsen, L.H., and Richoz, S., 2012, No causal link between terrestrial ecosystem change and methane release during the end-Triassic mass extinction: Geology, vol. 40, p. 531–534.

Lindström, S., and Erlström, M., 2006, The late Rhaetian transgression in southern Sweden: Regional (and global) recognition and relation to the Triassic–Jurassic boundary: Palaeogeography, Palaeoclimatology, Palaeoecology, vol. 241, p. 339–372.

Lund, J.J., 1977, Rhaetic to Lower Liassic palynology of the onshore south-eastern North Sea Basin: Danmarks Geologiske Undersøgelse II Række, vol. 109, p. 1–129.

Mader, D., 1992, Evolution of palaeoecology and palaeoenvironment of Permian and Triassic fluvial basins in Europe: Stuttgart, New York, Gustav Fischer Verlag, 783 p.

Michalík, J., Birŏn, A., Lintnerová, O., Götz, A.E., and Ruckwied, K., 2012, Climate change at the Triassic/Jurassic boundary in the northwestern Tethyan realm, inferred from sections in the Tatra Mountains (Slovakia): Acta Geologica Polonica, vol. 60, p. 535–548.

Milàn, J., Clemmensen, L.B., and Bonde, N., 2007, Vertical sections through dinosaur tracks (Late Triassic lake deposits, East Greenland) – undertracks and other subsurface deformation structures revealed: Lethaia, vol. 37, p. 285–296.

Montenat,, C., Barrier, P., Ott d´Estevou, P., and Hibsch, C., 2007, Seismites: An attempt at critical analysis and classification: Sedimentary Geology, vol. 196, p. 5-30.

Muller, A., 1974, Die Trias–Lias Grenzschichten Luxemburgs: Veröffentlichungen des Luxemburger Geologischen Dienstes, Luxembourg, Vol. 23, p. 1-89.

Nielsen, L.H., 2003, Late Triassic–Jurassic development of the Danish Basin and the Fennoscandian Border Zone, southern Scandinavia: Geological Survey of Denmark and Greenland Bulletin, vol. 1, p. 459–526.

Owen, G., 1996, Experimental soft-sediment deformation: structures formed by liquefaction of unconsolidated sands and some ancient examples: Sedimentology, vol. 43, p. 279-293.

Pálfy, J., Demény, A., Haas, J., Carter, E.S., Görög, Á., Halász, D., Oravecz-Scheffer, A., Hetényi, M., Márton, E., Orchard, M.J., Ozsvárt, P., Vető, I., and Zajzon, N., 2007, Triassic–Jurassic boundary events inferred from integrated stratigraphy of the Csővár section, Hungary: Palaeogeography, Palaeoclimatology, Palaeoecology, vol. 244, p. 11–33.

Pieńkowski, G., Niedźwiedzki, G., and Waksmundzka M., 2012, Sedimentological, palynological and geochemical studies of the terrestrial Triassic–Jurassic boundary in northwestern Poland: Geological Magazine, vol. 149, p. 308–332.

Rauscher, R., Hilly, J., Hanzo, M., and Marchal, C., 1995, Palynologie des couches de passage du Trias supérieur au Lias dans L'Est du Bassin Parisien. Problèmes de datation du « Rhétien » de Lorraine: Sciences Géologiques, vol. 48, p. 159–185.

Troedsson, G., 1951, On the Höganäs series of Sweden (Rhaeto–Lias) : Lunds Universitets Årskskrift Ny Följd, vol. 2, p. 1–269.

Vajda, V., Calner, M., and Ahlberg, A., 2013, Palynostratigraphy of dinosaur footprint-bearing deposits from the Triassic–Jurassic boundary interval of Sweden: GFF, vol.135, p. 120–130.

van de Schootbrugge, B., Quan, T.M., Lindström, S., Püttmann, W., Heunisch, C., Pross, J., Fiebig, J., Petschick, R., Röhling, H.-G., Richoz, S., Rosenthal, Y., and Falkowski, P.G., 2009, Floral changes across the Triassic/Jurassic boundary linked to flood basalt volcanism: Nature Geoscience, vol. 2, p. 589–594.

Legend to supplementary figures and table

Figure DR1. *(A)* Map of the Danish Basin and northernmost German Basin (southern Sweden, Denmark, northernmost Germany) showing main localities and additional localities. *(B)* Map of the Stenlille structure showing the location of the Stenlille-1, -4, -5 and -6 wells. The contours show the depth to top Gassum Formation in meters below mean sea-level.

Figure DR2. A. Correlation of cores through the Triassic–Jurassic boundary section in the wells Stenlille–1 to Stenlille–6 (located in Fig. DR1). Five to eight horizons with soft sedimentation structures are seen in each core separated by thicker or thinner intervals of undisturbed sediments. The deformation structures are interpreted as caused by seismic chocks, and the disturbed sediments are interpreted as seismites. The sediments are referred to the Rhaetian Gassum Formation and the latest Triassic to Early Jurassic Fjerritslev Formation. The formation boundary follows a maximum flooding surface (MFS7, Nielsen 2003). The seismites are found within the grey siltstone interval, which also includes some very fine-grained sandstones. The presence of wave-ripples indicates deposition at depths close to storm wave-base. The grey siltstone interval corresponds largely to the *Ricciisporites–Polypodiisporites* Zone and to the end–Triassic mass-extinction (sees main text, Fig. 2). Depth in meters below Kelly Bushing. Legend in Fig. DR2, B.

B. Legend for Figs. DR2-3.

Figure DR3. Correlation from the Danish Basin (N Albert quarry, Stenlille wells), to the German Basin (Rødby–1, Schandelah), to the Paris Basin (Junglinster Heedhaff). In all three basins soft sediment deformations, interpreted as seismites, are frequent within sediments deposited just prior to and within the *Riciisporites–Polypodiisporites* Zone. The presence of soft sediment deformation structures throughout three basin, but virtually restricted to one biozone, strongly suggests that they were generated by regional events, such as earthquakes. All the sedimentological logs are simplified. The signatures are explained in Fig. DR2, B.

Figure DR4. Soft sediment deformation structures in the latest Rhaetian of the Danish Stenlille cores and the German Schandelah core. *(A)* Greenish grey heterolithic fine-grained sandstone with wedge-shaped crack, filled with greenish mudstone clasts a few mm in diameter, interpreted as active fill due to injection. The sandstone is dominated by wave-generated cross-lamination. Stenlille-1 1498.02–1498.21 m. *(B)* Same lithologies as in *A*, Stenlille-1 1497.33–1497.49 m**.** *(C)* Greenish grey heterolithic fine-grained sandstone with wave-generated cross-lamination overlain by slightly finer grained greenish sandstone with soft sediment deformation structures. These are attributed to liquefaction of the sediment induced by seismic shock. Older strata had a lower porosity and were not liquefied. Stenlille-1 1496.44–1496.60 m. *(D)* Structureless greenish grey sandstone with remnants of cross-lamination preserved in 'pockets' of paler sandstone, which subsided into the liquefied sediment. Liquefaction was induced by seismic shock. At the top of the core piece small slump-folds are present. Stenlille-1 1496.06–1496.35 m. *(E)* Irregular slump folds in very fine-grained greenish sandstone, attributed to liquefaction of the sediment induced by seismic shock. The underlying and overlying parts of the core are not disturbed. Stenlille-4 1507.65–1507.77 m. *(F)* Small, steeply dipping fault with irregular fault trace including formation of small horse, and satellite splays into soft sediment. The formation of the structures may have been hydrodynamically triggered and cored part may be part of a hydrodynamic breccia. Stenlille-4, 1505.5–1505.65 m. *(G)* Slump fold involving siltstone with numerous small clay clasts Stenlille-4, 1504.4–1504.6 m. *(H)* Cross-laminated, very fine-grained sandstone interrupted by 6 cm thick horizon of soft sediment deformation. The planar upper boundary indicates that the top of the deformation structures was eroded by the overlying cross-laminated sandstone. Stenlille-4, 1503.8–1503.9 m. *(I–L)* Examples of soft-sediment deformations in the Schandelah core. *(I)* Grey silt to fine-grained sand showing liquefaction, Schandelah 331.01–330.89 m. *(J)* Medium to dark grey fine sandstone with irregular cracks, 330.22–330.08 m. *(K)* Medium to dark grey fine-grained sandstone with soft-sediment deformation structures, 327.16–327.02 m. *(L)* Medium to dark grey fine-grained sandstone with soft-sediment deformation structures, 322.15–322.02 m.

Figure DR5. Examples of soft sediment deformation structures in the Junglinster Heedhaff section and the Grouft core. *(A–C)* Grouft drillcore (Luxembourg): Reddish brown silt streaked, laminated clays with different types of microslumps. *(A)* Core depth 91.55m–91.72m, vertical scale 15cm. *(B)* Core depth 92.42m–92.50m, vertical scale 8cm. *(C)* Core depth 92.68m – 92.78m, vertical scale 10cm. *(D–E)* Outcrop section at Junglinster Heedhaff (Luxembourg): *(D)* Dark grey conglomeratic sand/clay at the base, injected into laminated light grey clay (forming veins and flame structures in the middle part). In the upper part laminated clay/silt is slumped and horizontally folded (2.20m–2.35m). Knife for scale is 10cm long. *(E)* Disturbed clay-quartzite alternation at the base, microfolded and sheared at the top of the sample (1.50m).

Table DR1. NAA analysis of samples straddling the soft sediment deformation interval at N Albert quarry.

Author contributions: SL, BvdS and GKP, designed the project, executed the research and wrote the paper. The palynological data from Stenlille were generated by SL and KD, and from Schandelah by BvdS. SL generated the palynological data from N Albert. GKP performed the sedimentology of the Stenlille wells and N Albert. LHN performed geophysical log-correlations between the Stenlille wells. SL, GKP, LJ, RWH and CA analysed and interpreted the inorganic geochemistry from the Swedish and Danish sites. CA checked for shocked metamorphic features. HIP performed organic petrology on the coals from N Albert. KHH performed sedimentology and palynology on the Rødby-1 core. ME performed the core description and sedimentology of the Swedish sites mentioned in the supplement. CT contributed with interpretation and general context of large igneous provinces. SL, GKP, KD, RWH, LJ, KHH, CA and LHN participated in the fieldwork at N Albert quarry. NK and JT performed the sedimentology of the two Luxembourg sites. All authors contributed to the text.

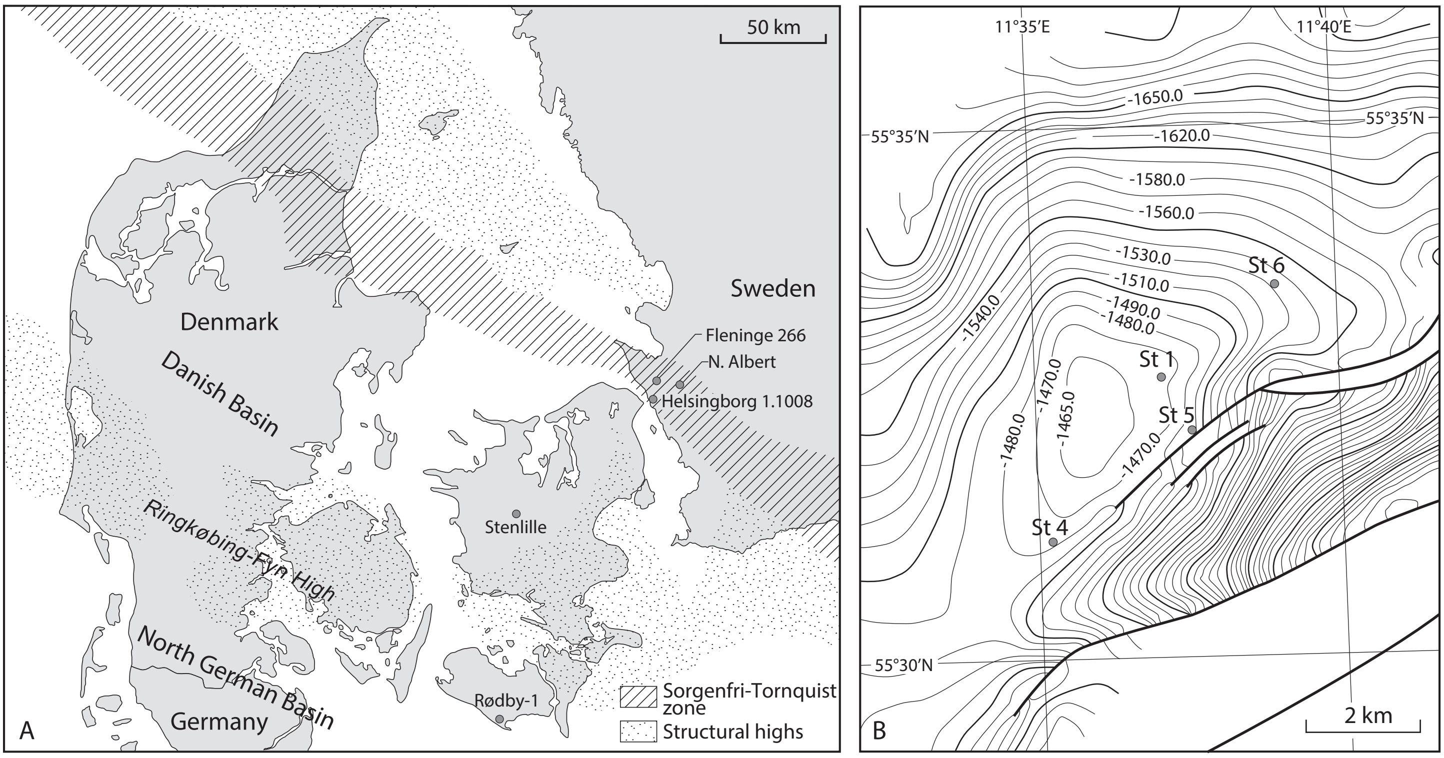
50 km
Sweden
Denmark
Danish Basin
Fleninge 266
N. Albert
Helsingborg 1.1008
Stenlille
Ringkøbing-Fyn High
North German Basin
Germany
Rødby-1
Sorgenfri-Tornquist zone
Structural highs
A
11°35'E
11°40'E
55°35'N
55°35'N
55°30'N
-1650.0
-1620.0
-1580.0
-1560.0
-1530.0
-1510.0
-1490.0
-1480.0
-1540.0
-1470.0
-1465.0
-1480.0
-1470.0
St 1
St 4
St 5
St 6
2 km
B

Fig DR 1

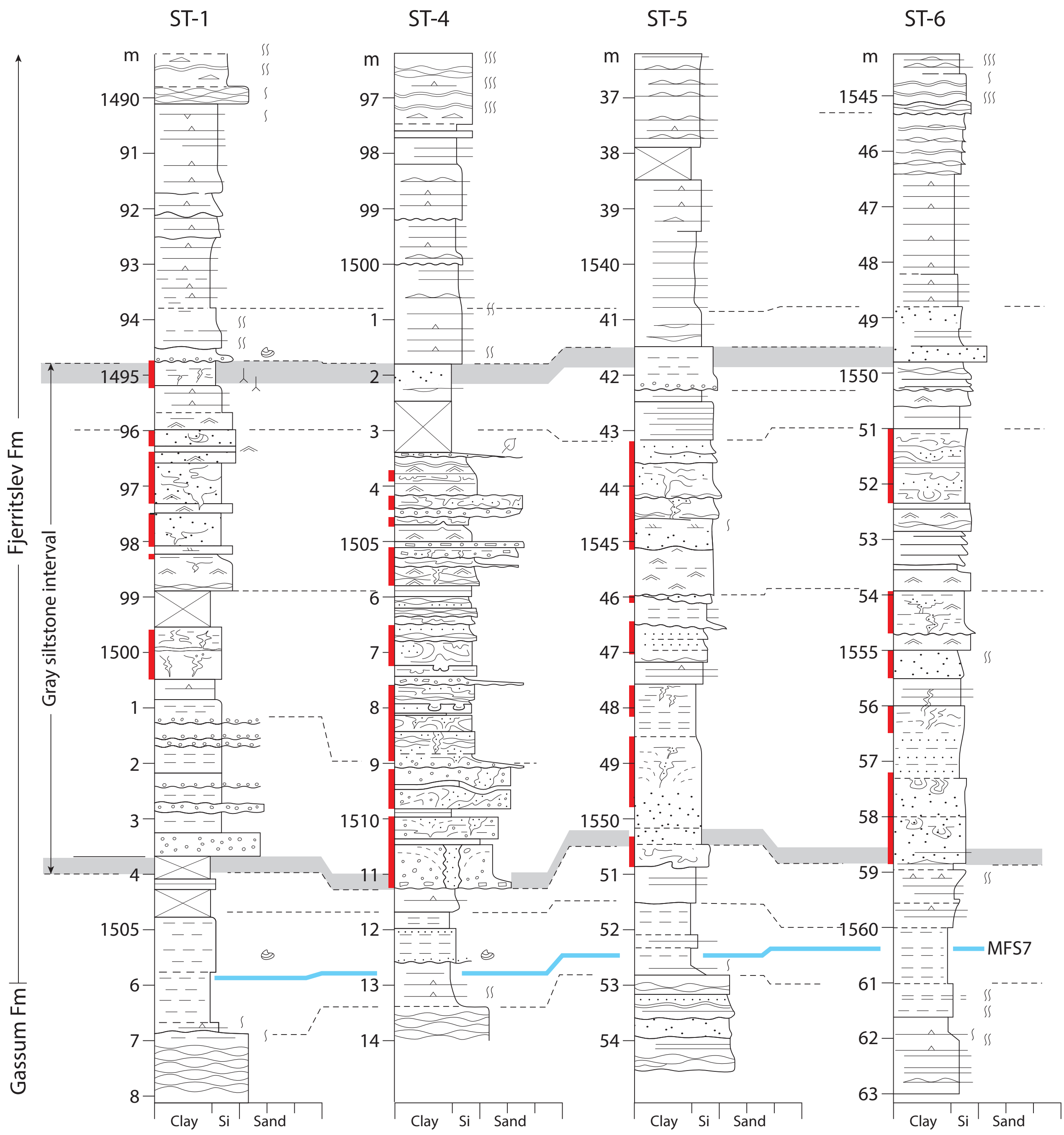

ST-1
ST-4
ST-5
ST-6
Fjerritslev Fm
Gassum Fm
Gray siltstone interval
MFS7
Clay
Si
Sand

Fig DR 2A

N Albert, Rødby-1
Stenlille1, 4-6

Lithology

- Coal
- Coal clasts
- Clay clasts
- Concretion

Sedimentary structures

- Lamination
- Weak lamination
- Undulatory lamination
- Sand-or silt-streak
- Lenticular bedding
- Wavy bedding
- Cross-lamination
- Wave-ripple cross-lamination
- Planar cross-bedding
- Trough cross-bedding
- Hummocky cross-stratification
- Hummocky cross-stratification
- Structureless
- Soft sediment deformation structures

Trace fossils and biota

- Weak to intense bioturbation
- Bivalve
- Rootlet
- Interval with soft sediment deformation
- Not exposed

Junglinster Heedhaff

Lithology

- Mudstone
- Calcareous mudstone
- Dolomite limestone
- Silt- and sand-streaks
- Sandstone
- Conglomerate
- Bivalves
- Shell layer

Sedimentary structures

- Disturbed sediments
- Water escape structures

Trace fossils and biota

- Placodus bones
- Erosional boundary

Schandelah

Lithology

- Sandstones
- Laminated claystones
- Paper shales
- Silt- and claystones
- Siderite concretions
- Clay clasts / rip-ups

Sedimentary structures

- Slump folds
- Cross-lamination
- Through cross-bedding
- Structureless
- Mud-draped bedform
- Liquefaction
- Syneresis cracks
- Seismite?

Fig DR 2B

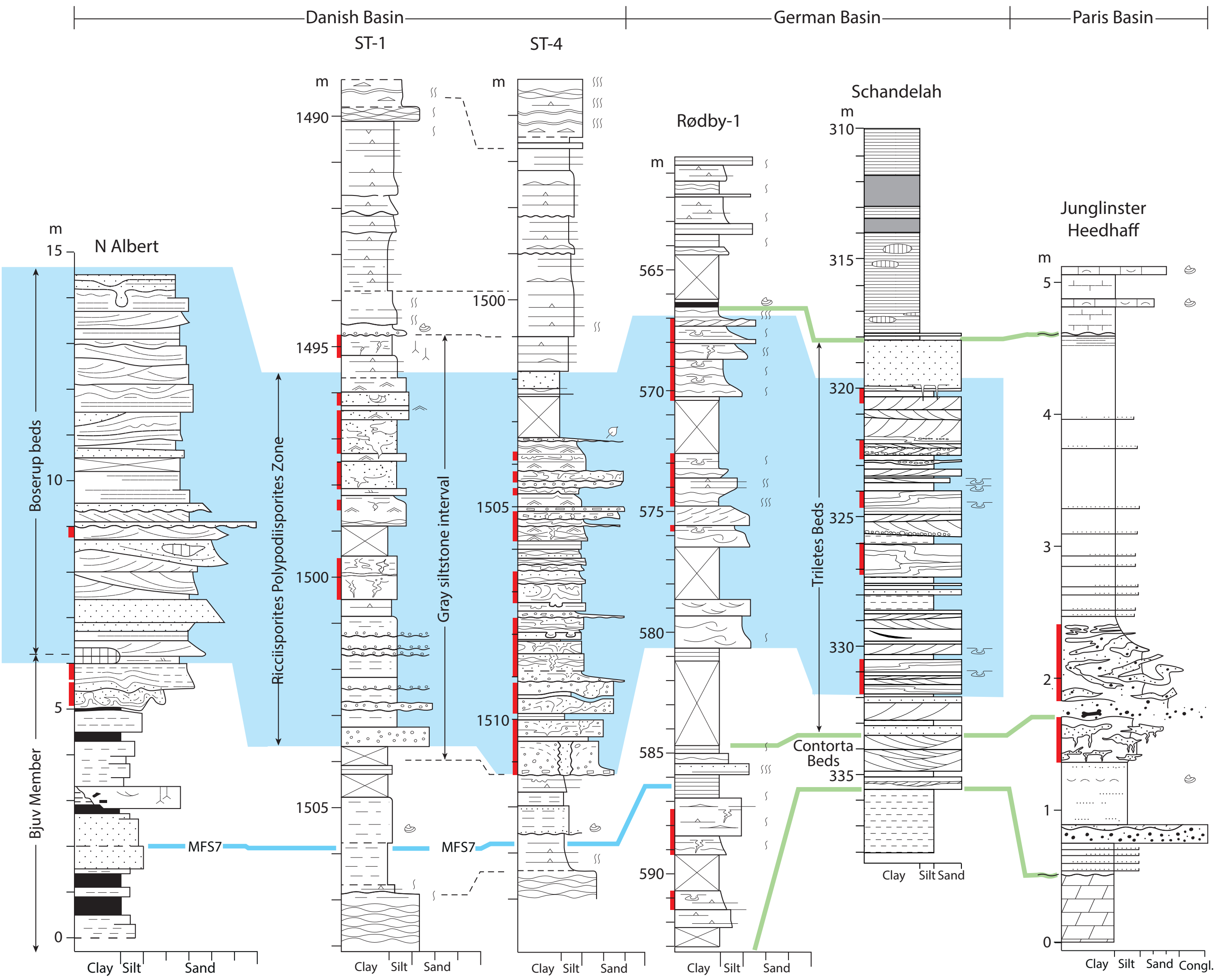

Danish Basin
German Basin
Paris Basin
ST-1
ST-4
N Albert
Rødby-1
Schandelah
Junglinster Heedhaff
Boserup beds
Bjuv Member
Ricciisporites Polypodiisporites Zone
Gray siltstone interval
Triletes Beds
Contorta Beds
MFS7
MFS7
Clay Silt Sand
Clay Silt Sand
Clay Silt Sand
Clay Silt Sand
Clay Silt Sand
Clay Silt Sand Congl.

Fig DR 3

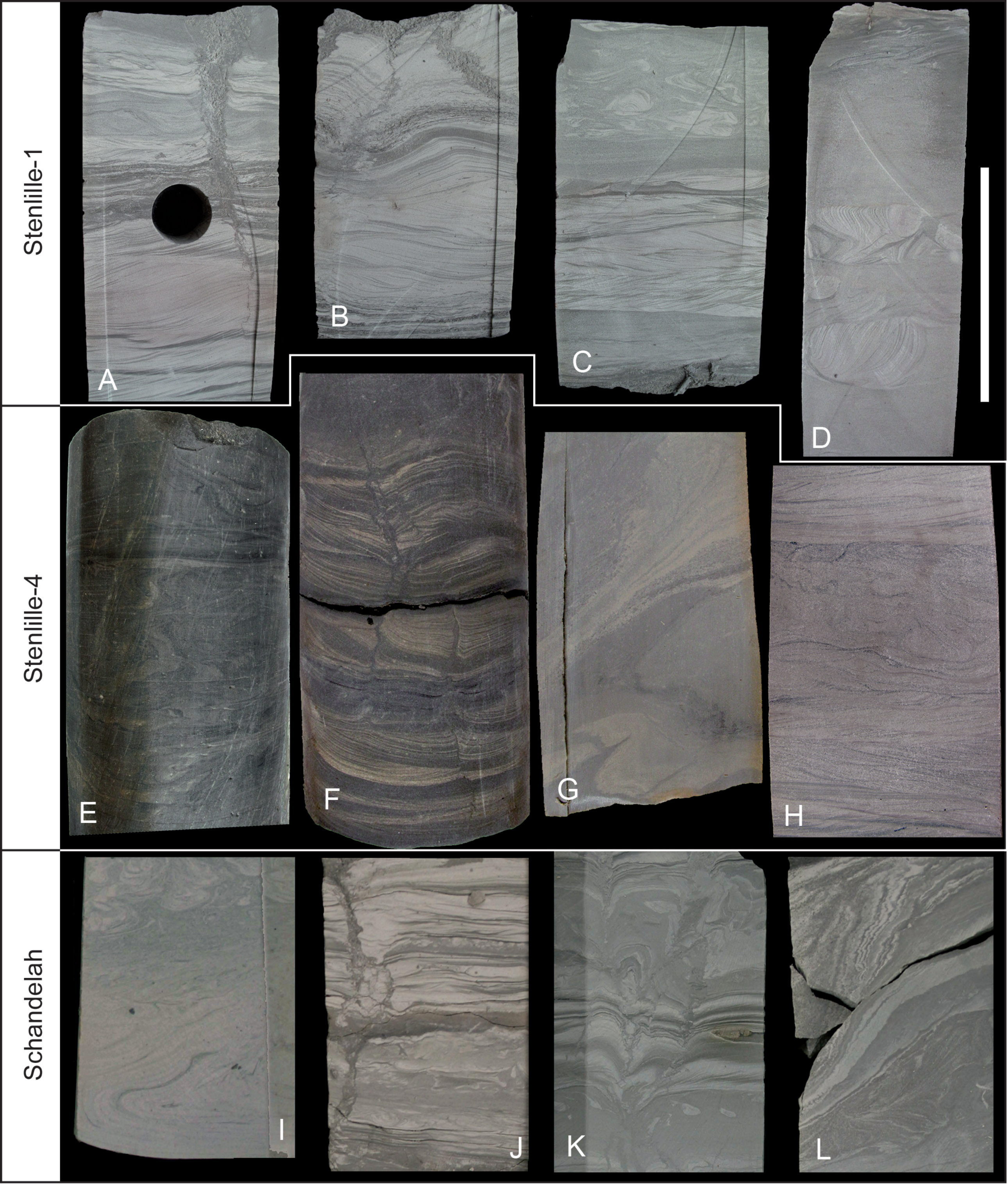

Fig DR 4

Figure DR6. Soft sediment deformation structures in the Junglinster Heedhaff section and the Grouft core.

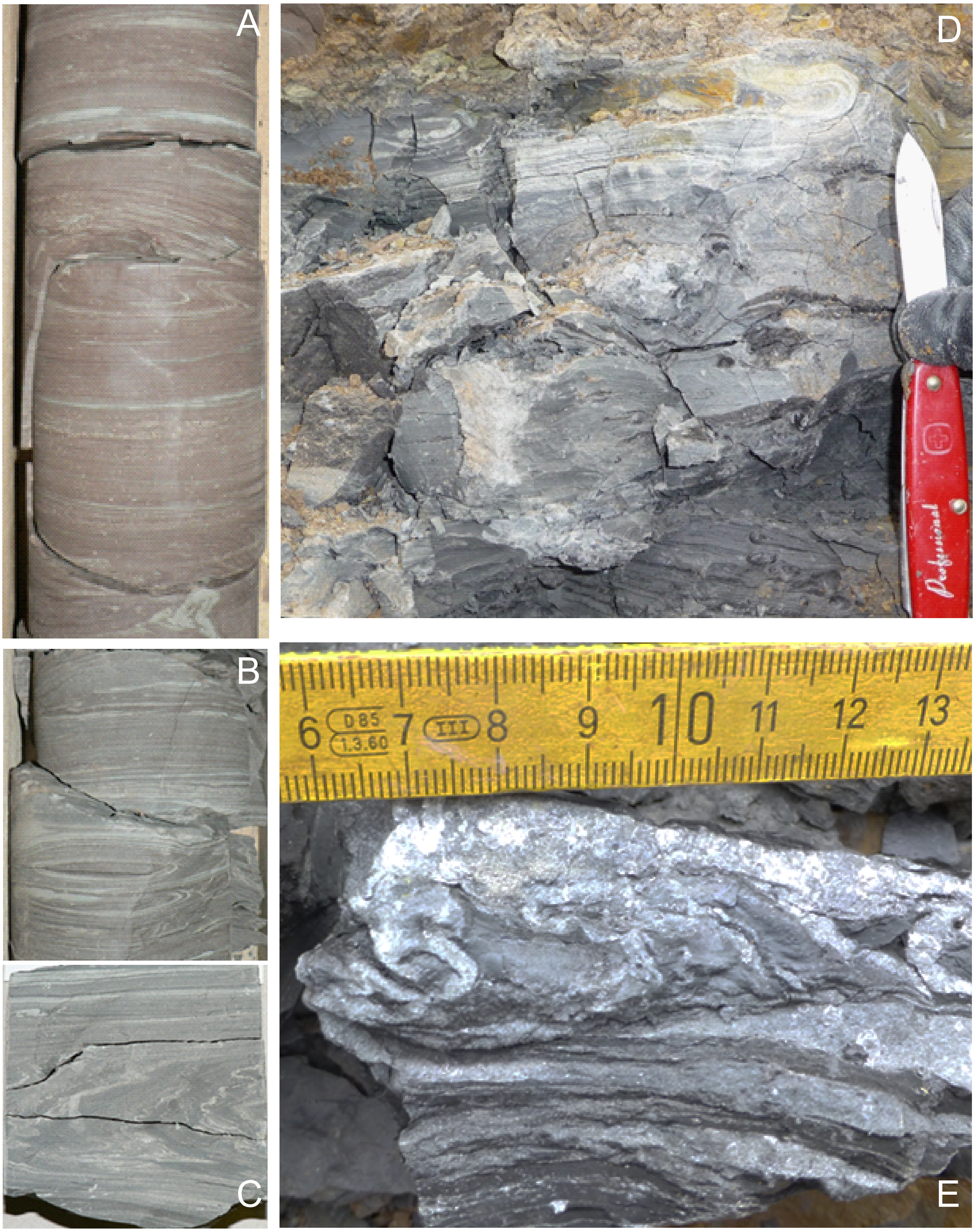

Fig DR 5

Table DR1. NAA analysis of samples straddling the soft sediment deformation interval at N Albert quarry.

Sample nr	Height (m)	Comment	Weight (grams)	Au (ppb)	Ir (ppb)	Os (ppb)	Pd (ppb)	Pt (ppb)	Rh (ppb)	Ru (ppb)
519556	6,7		20,00	<1	<1	<10	<20	<20	<5	<50
516843	5,4		20,00	<1	<1	<10	<20	<20	<5	<50
516842	5,1		20,00	<1	<1	<10	<20	<20	<5	<50
516841	4,8	seismite 1	20,00	1	<1	<10	<20	<20	<5	<50
516807	4,8	seismite 1	20,00	<1	<1	<10	<20	<20	<5	<50
516840	4,8	top claystone below seismite	20,00	4	<1	<10	<20	<20	<5	<50
516839	4,6		20,00	3	<1	<10	<20	<20	<5	<50
516838	4,52		10,00	3	<1	<10	<20	<20	<5	<50
516837	4,3		20,00	2	<1	<10	<20	<20	<5	<50
516836	4,08		20,00	5	<1	<10	<20	<20	<5	<50
516835	3,33		20,00	3	<1	<10	<20	<20	<5	<50
516834	3,03		20,00	1	<1	<10	<20	<20	<5	<50
516833	2,1		20,00	3	<1	<10	<20	<20	<5	<50
516832	1,88		20,00	2	<1	<10	<20	<20	<5	<50
516831	1,7		20,00	2	<1	<10	<20	<20	<5	<50
516830	1,5		20,00	2	<1	<10	<20	<20	<5	<50
516829	1,12		20,00	2	<1	<10	<20	<20	<5	<50
516828	-0,1		10,00	3	<1	<10	<20	<20	<5	<50
516827	-0,2		10,00	3	<1	<10	<20	<20	<5	<50
516826	-0,3		20,00	2	<1	<10	<20	<20	<5	<50